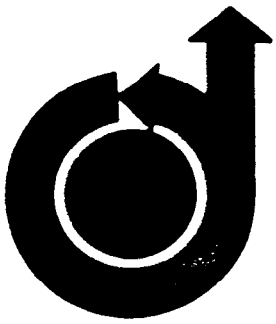

AIAA Paper No. 73-746

MODELING THE EFFECT OF AIR AND OIL UPON THE THERMAL RESISTANCE OF A SPHERE-FLAT CONTACT

by
M. MICHAEL YOVANOVICH and W. W. KITSCHA
University of Waterloo
Waterloo, Ontario

AIAA 8th Thermophysics Conference

PALM SPRINGS, CALIFORNIA / JULY 16-18, 1973

MODELING THE EFFECT OF AIR AND OIL UPON THE THERMAL RESISTANCE OF A SPHERE-FLAT CONTACT

M. Michael Yovanovich* and W. W. Kitscha**
Thermal Engineering Group
University of Waterloo
Waterloo, Ontario

Abstract

An analysis is presented for predicting the overall thermal resistance of sphere-flat contacts as a function of solid constriction resistance based upon elasticity theory, radiative heat transfer and conductive resistance of the gas gap as a function of gas pressure ranging from vacuum to atmospheric conditions. Both coupled and decoupled solid/gas conduction heat transfer models are considered. The effect of oil, with and without gas present, is considered. Excellent agreement is observed between the theory and test data based upon air and argon over the gas pressure range from 10^{-5} mm Hg to atmospheric conditions for two different spherical specimens.

Nomenclature

A = heat transfer area
a = contact radius
D = sphere diameter
D_e = gas layer thickness
E = modulus of elasticity
F = direct view factor between black surfaces
$\bar{F}$ = view factor between black surfaces with reradiating surfaces
$\bar{f}$ = view factor between grey surfaces with reradiating surfaces
G_1 = integral for gas resistance under continuum conditions, Eq. (24)
G_o = integral for oil resistance, Eq. (35)
G_2 = integral for gas resistance in slip and transition regimes, Eq. (41)
K = complete elliptic integral of the first kind
Kn = Knudsen number (Λ/δ)
k = thermal conductivity
k_g^* = dimensionless gas conductivity (k_g/k_s)
k_o^* = dimensionless oil conductivity (k_o/k_s)
$k_{g\infty}^*$ = dimensionless gas conductivity under continuum conditions ($k_{g\infty}/k_s$)
L = dimensionless contact parameter, Eq. (1)
m = contact size parameter
N = normal contact load
n = contact size parameter
P_g = gas pressure (mm Hg)
P_g^* = dimensionless gas pressure ($760/P_g$)
Q = heat flow rate (W)
R = thermal resistance ($^oK/W$)
R^* = dimensionless thermal resistance ($Dk_s R$)
R_c^* = dimensionless constriction resistance
R_g^* = dimensionless gas resistance
R_o^* = dimensionless oil resistance
R_r^* = dimensionless radiative resistance
R_t^* = dimensionless total resistance
r = radial coordinate
T = absolute temperature (^oK)
T_c = contact temperature, Eq. (25)
T^* = dimensionless absolute temperature ($T/288$)
x = dimensionless radial position (r/a)
z = coordinate normal to contact plane

Greek Symbols

α = accommodation coefficient
β = lower limit for gas with oil present, Eqs. (23) and (35)
γ = upper limit for gas in slip and transition regimes, Eq. (43)
ξ = lower limit of integration for oil or air
δ = gas gap thickness, Eq. (2) or Eq. (3)
ε = emissivity
κ^2 = argument for complete elliptic integral, Eq. (6)
Λ = mean free path of gas
ν = Poisson's ratio
π = Pi
ρ = radius of curvature of contacting solids
ρ^* = radius of curvature of contact, Eq. (7)
σ = Stefan-Boltzmann constant
ψ^* = thermal constriction parameter, Eq. (6)

Subscripts

1 = sphere
2 = flat
3 = reradiating surfaces
∞ = continuum

* Professor of Mechanical Engineering, University of Waterloo, Member AIAA.

** NRC Graduate Research Assistant, Atomic Energy of Canada, Ltd., Sheridan Park, Ontario.

c = constriction
g = gas
o = oil
r = radiation
s = harmonic mean value of conductivity, Eq. (5)
t = total

Introduction

Heat transfer across bearings is of great interest to those thermal engineers who are responsible for the thermal design of spacecraft. Jansson[1] obtained experimental data for dry and lubricated instrument bearings in a vacuum. Yovanovich[2-4] developed a general constriction resistance theory for contacting paraboloids which agreed with the vacuum test data obtained with unlubricated instrument bearings. This theory was based upon negligible radiation effects and no contribution to heat transfer due to air or oil. This paper is an extension of that theory to include radiation effects as well as gas conduction over the pressure range of one atmosphere to 10^{-5} mm Hg. The effect of an oil with and without air present is also considered. The theory is compared with test data obtained for a sphere in elastic contact with a flat.

Analysis

Problem Statement

Consider the thermal resistance to heat transfer across the sphere-flat contact shown in Fig. 1. Heat can be transmitted across the contact plane in the following ways: a) conduction through the contact area, b) radiative transfer across the gap between the sphere and flat outside the contact area, c) conduction through the gas which may be present in the gap, d) conduction through a fluid such as oil which may be present in a portion of the gap, Fig. 1b, and e) convective effects within the gas under special conditions. If all these mechanisms are independent of each other and are present simultaneously, they can be considered to be thermally connected in parallel; i.e., a decoupled model is assumed.

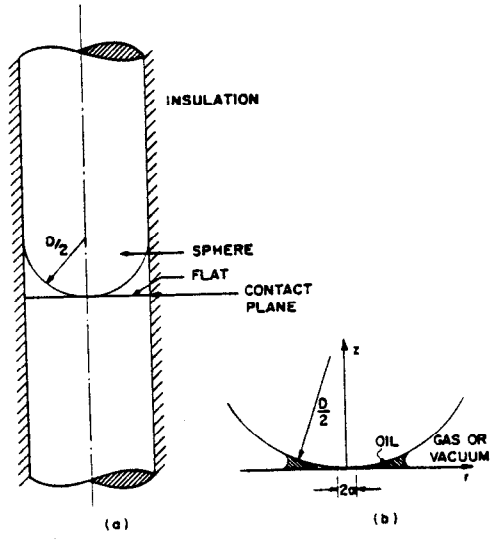

Fig. 1 Schematic of flat-sphere contact

This paper will consider thermal constriction resistance due to the heat flow through the contact area, radiative resistance across the gap, conductive gas resistance based upon coupled and decoupled models for gas pressures ranging from vacuum (10^{-5} mm Hg) up to atmospheric conditions, and conductive resistance due to a fluid region. Free convection is assumed to be negligible.

System Geometry

Consider the contact between a smooth sphere of diameter D and a smooth flat surface, Fig. 2. For convenience the coordinates (r, z) are chosen with the origin placed in the center of the contact area. The two important geometric parameters: contact radius a and local gap thickness δ can be calculated by means of the following expressions derived from elasticity theory:[5]

$$\frac{2a}{D} = \left[\frac{3N}{D^2}\left(\frac{1-\nu_1^2}{E_1} + \frac{1-\nu_2^2}{E_2}\right)\right]^{1/3} \qquad (1)$$

Here N is the normal contact load, while E_1, E_2 and ν_1, ν_2 are the elastic properties of the sphere and flat.[2] The dimensionless contact parameter D/2a

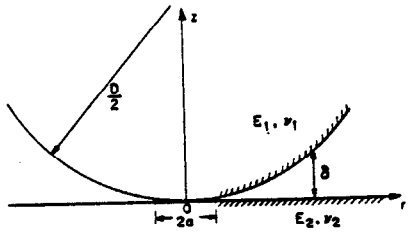

Fig. 2 Schematic of elastic contact and gap thickness

will be denoted by L, which for a fixed system depends only upon the contact load. For the local gap thickness we have from elasticity theory[6]

$$2\frac{\delta}{D}L^2 = \left\{\frac{2}{\pi}\sin^{-1}\frac{1}{x} - 1\right\}\left\{1 - \frac{x^2}{2}\right\} + \frac{1}{\pi}\sqrt{x^2 - 1} \qquad (2)$$

where $x \equiv r/a$ and L is given by Eq. (1). Eq. (2) includes the overall displacement of the sphere under the load N. There is a simpler geometric expression which neglects the bulk deformation of the sphere:

$$2\frac{\delta}{D}L = \sqrt{L^2 - 1} - \sqrt{L^2 - x^2} \qquad (3)$$

which is comparable to Eq. (2) for most values of L and is amenable to integration. Eq. (3) will be used throughout this paper whenever thermal resistance of the air or oil is considered.

Thermal Resistances

Constriction Resistance

In the analyses to follow it will be assumed that the heat flow rate through the contact area is always present and independent of the heat flow rates through the gas, through the oil and across the gap by means of radiation. The assumption is clearly valid for the extreme case of a dry con-

tact under vacuum conditions when only constriction and radiation resistances are present. The assumption is probably a good approximation for the other extreme case of a lubricated contact under atmospheric conditions.

It is further assumed that the general constriction resistance expression developed by Yovanovich for contacting smooth paraboloids[4] is applicable for all conditions provided surface roughness effects are negligible:

$$k_s R_c = \frac{\psi^* [1/\rho^*]^{1/3}}{2\left[\frac{3N}{2}\left(\frac{1-\nu_1^2}{E_1} + \frac{1-\nu_2^2}{E_2}\right)\right]^{1/3}} \tag{4}$$

where the harmonic mean thermal conductivity k_s of the contacting solids is usually written as

$$k_s = 2\, k_1 k_2/(k_1 + k_2) \tag{5}$$

The constriction parameter ψ^* can be evaluated by means of the following expression[4]:

$$\psi^* = \frac{2}{\pi}\frac{K(\kappa^2)}{m} \tag{6}$$

where K is the complete elliptic integral of the first kind of modulus $\kappa^2 = 1 - (n/m)^2$; m and n are dimensionless geometric parameters[5] which are functions of the geometry of the contacting paraboloids. The geometric parameter ρ^* is defined as[5]

$$\frac{1}{\rho^*} = \frac{1}{\rho_1} + \frac{1}{\rho_1'} + \frac{1}{\rho_2} + \frac{1}{\rho_2'} \tag{7}$$

where ρ_1, ρ_1' are the principal radii of curvature for solid 1 and ρ_2, ρ_2' are the principal radii of curvature for solid 2. Eq. (4) assumes a very simple form whenever a sphere ($\rho_1 = \rho_1' = D/2$) is in contact with a flat ($\rho_2 = \rho_2' = \infty$). For this special case of contacting paraboloids, $\psi^* = 1$[8] because $K(\kappa^2) = \pi/2$ and $m = n = 1$. Also ρ^* becomes simply D/2, and, therefore, Eq. (4) reduces to[4]

$$k_s R_c = \frac{1}{\left[3ND\left(\frac{1-\nu_1^2}{E_1} + \frac{1-\nu_2^2}{E_2}\right)\right]^{1/3}} \tag{8}$$

Multiplying through by the sphere diameter to nondimensionalize Eq. (8), we obtain

$$Dk_s R_c = R_c^* = L \tag{9}$$

where L is the dimensionless loading parameter defined by Eq. (1).

Radiative Resistance

Consider the radiation heat transfer between a hemispherical surface having emissivity ε_1 and a flat disc having emissivity ε_2, completely enclosed by a reradiating surface ε_3 as shown schematically in Fig. 3. To make the problem tractable the hemispherical surface and the flat are assumed to be isothermal having temperatures T_1 and T_2, respectively. According to the Stefan-Boltzmann Law, the net radiative heat transfer between the hemisphere and the flat in the presence of reradiating

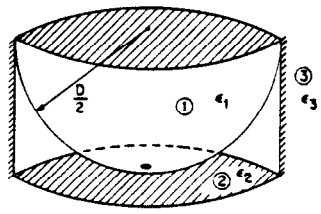

Fig. 3 Model for radiation resistance

surfaces is given by

$$Q_r = A_1 \bar{\mathcal{F}}_{12}\, \sigma\, [T_1^4 - T_2^4] \tag{10}$$

where the heat transfer area is $A_1 = (\pi D^2/4)[1 - 1/L^2]$. The grey-body view factor $\bar{\mathcal{F}}_{12}$ for the enclosure shown in Fig. 3 can be determined by means of the following expression[9]:

$$\frac{1}{\bar{\mathcal{F}}_{12}} = \frac{1-\varepsilon_1}{\varepsilon_1} + \left(\frac{A_1}{A_2}\right)\left[\frac{1-\varepsilon_2}{\varepsilon_2}\right] + \frac{1}{\bar{F}_{12} + \left\{\frac{1}{\bar{F}_{13}} + \left(\frac{A_1}{A_2}\right)\frac{1}{\bar{F}_{23}}\right\}^{-1}} \tag{11}$$

In Eq. (11), $\bar{F}_{12}$, $\bar{F}_{13}$ and $\bar{F}_{23}$ are the view factors between black surfaces in the presence of reradiating surfaces. The direct view factor between a hemisphere and a disc which are in point contact is[10]

$$F_{21} = \frac{1}{2}\left[1 - \frac{1}{\sqrt{2}}\right] \tag{12}$$

It will be assumed that Eq. (12) is valid for contacting surfaces provided $L \geq 10$. Using the reciprocity relationship:

$$A_1 F_{12} = A_2 F_{21} \tag{13}$$

the direct view factor F_{12} can be evaluated. Having determined, for the system shown in Fig. 3, that $\bar{F}_{12} = 0.586$, $\bar{F}_{13} = 0.414$ and $\bar{F}_{23} = 0.707$, it can be easily shown that Eq. (11) yields[11]

$$\frac{1}{\bar{\mathcal{F}}_{12}} = \frac{1-\varepsilon_1}{\varepsilon_1} + \frac{1-\varepsilon_2}{2\varepsilon_2} + 0.5766 \tag{14}$$

For moderate temperature drops across the gap, the radiative resistance for $L \geq 10$ can be approximated as

$$R_r = \frac{1}{A_1 \bar{\mathcal{F}}_{12}\, 4\sigma\, T_m^3} \tag{15}$$

where T_m is the mean absolute temperature of the gap. Using $A_1 = \pi D^2/4$ and Eq. (14), the dimensionless expression for the radiative resistance can be written as

$$Dk_s R_r = R_r^* = \frac{k_s \left[\frac{1-\varepsilon_1}{\varepsilon_1} + \frac{1-\varepsilon_2}{2\varepsilon_2} + 0.5766 \right]}{\pi D \sigma T_m^3} \quad (16)$$

Total Resistance Under Vacuum Conditions

If we assume that the constriction resistance and the radiative resistance are thermally connected in parallel, the total resistance under vacuum conditions with no oil present is simply

$$\frac{1}{R_t} = \frac{1}{R_c} + \frac{1}{R_r} \quad (17)$$

Multiplying each term by $1/Dk_s$ to non-dimensionalize, and after rearranging, we obtain

$$R_t^* = L/(1 + L/R_r^*) \quad (18)$$

for the dimensionless total resistance under vacuum conditions including radiative effects.

Gas Conduction Under Continuum Conditions (Kn → 0)

The resistance to conduction heat transfer through the gas gap under atmospheric pressure is very complex because the solid boundaries are not isothermal, and the local gap thickness varies monotonically from a value of zero adjacent to the contact area (x = 1) to practically the radius of the contacting sphere at the outer region of the contact plane (x = L). If we define a local pseudo-Knudsen number as the ratio of the mean free path of the gas corresponding to the average gas temperature and pressure within the gas gap to the local gas gap thickness

$$Kn = \frac{\Lambda}{\delta} \quad (19)$$

it can be shown that after substituting Eq. (3) for δ into Eq. (19), the following expression:

$$\xi = \frac{x}{L} = 2\sqrt{\frac{\Lambda}{DKn}}\sqrt{1 - \frac{\Lambda}{DKn}} \quad (20)$$

relates the dimensionless radial position to Λ/D which is the maximum value of the local pseudo-Knudsen number based upon the diameter of the hemisphere and Kn. The mean free path Λ at any temperature and pressure can be determined from[13]

$$\Lambda = \Lambda_\infty \left(\frac{T}{288}\right)\left(\frac{760}{P_g}\right) \quad (21)$$

where Λ_∞ is the mean free path under atmospheric conditions. For air at 15°C, $\Lambda_\infty = 6.40 \times 10^{-6}$ cm.[13]

It is customary when considering heat transfer through a gas layer bounded by infinitely large, parallel, isothermal walls to assume continuum conditions to prevail throughout the gas layer and also within the gas volume adjacent to the wall provided the Knudsen number is much smaller than unity, i.e., Kn < 0.01. If this value of Kn is used in Eq. (20), with D = 2.54 cm, L = 100, and T^* and P_g^* both equal to unity, it can be shown that x = 3.2. This means that the gas gap region between x = 1 and x = 3.2 cannot be treated as a continuum, and only the region $3.2 < x \leq L$ can be so considered.

In both decoupled and coupled models it will be assumed that there exists a region adjacent to the contact area which must be excluded when considering gas conduction through a continuum. In both models it will be assumed that the gas conductivity is uniform throughout the entire gas gap region considered to be a continuum. It will be assumed that the heat conducted through the gas flows within annular regions bounded by adiabatic walls which are perpendicular to the contact plane, Fig. 4.

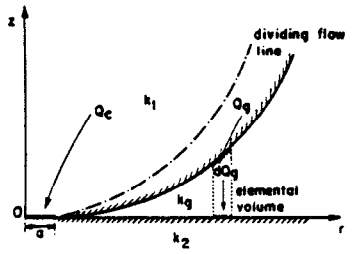

Fig. 4 Model for gas resistance

Decoupled Model

In this model it will be assumed that the solid surfaces are isothermal, therefore the conduction resistance of an elemental volume of gas having local thickness δ and flow area 2πrdr is simply

$$dR_g = \frac{\delta}{k_g 2\pi r dr} \quad (22)$$

where k_g is the gas conductivity. After substitution of Eq. (3) for δ, non-dimensionalizing, and integrating from $x = \xi > 1$ to x = L, one obtains

$$\frac{1}{R_g^*} = \frac{1}{Dk_s R_g} = k_g^* G_1(L,\xi) \quad (23)$$

where the integral in Eq. (23) is defined as

$$G_1(L,\xi) = \frac{\pi}{L}\sqrt{L^2-1}\ln\left(\frac{\sqrt{L^2-1}}{\sqrt{L^2-1}-\sqrt{L^2-\xi^2}}\right) - \sqrt{L^2-\xi^2} \quad (24)$$

where L is the dimensionless loading parameter, Eq. (1), and ξ is the lower limit of integration based upon the definition of the local pseudo-Knudsen number, Eq. (19).

Coupled Model

This model considers the coupling of the heat flow rate through the contact area, Q_c, called the primary flow rate and the heat flow rate through the gas, Q_g, called the secondary flow rate. In this model it is hypothesized that the temperature distributions over the hemispherical surface and the flat are determined by the heat flow rate

through the contact area and the corresponding thermal constriction resistance. It is further assumed that the constriction resistance of the solid with gas present in the gap is practically identical to the solid resistance with no gas present, i.e., under vacuum conditions. These assumptions are certain to be valid when the contact area is large and the constriction resistance is small relative to the gas resistance. The temperature distribution over the surface of the flat under vacuum conditions is according to Yovanovich[7]

$$T_c - T_2 = [Q_c/2\pi k_2 a] \tan^{-1} \sqrt{(r/a)^2 - 1} \qquad (25)$$

where T_c is the uniform temperature of the contact area, T_2 is the surface temperature at any position r and k_2 is the thermal conductivity of the solid. The heat flow is into the flat. As a first approximation it will be assumed that over the surface of the hemisphere one can write a similar expression

$$T_1 - T_c = [Q_c/2\pi k_1 a] \tan^{-1} \sqrt{(r/a)^2 - 1} \qquad (26)$$

where clearly the heat flows out of the hemisphere. Adding Eqs. (25) and (26) yields

$$T_1 - T_2 = [Q_c/\pi k_s a] \tan^{-1} \sqrt{(r/a)^2 - 1} \qquad (27)$$

which is the local temperature drop across the gas gap. The harmonic mean thermal conductivity is defined by Eq. (5). According to Fourier the elemental heat flow rate through the annular region is given by

$$dQ_g = k_g \frac{(T_1 - T_2)}{\delta} 2\pi r dr \qquad (28)$$

Upon substitution of Eq. (3) for δ, Eq. (27) for $(T_1 - T_2)$, non-dimensionalizing and then integrating from $x = \xi > 1$ to $x = L$, one obtains the following relationship between the solid and gas heat flow rates:

$$\frac{1}{2} \left(\frac{Q_g}{Q_c}\right) \left(\frac{k_s}{k_g}\right) = \int_{\xi}^{L} \frac{x \tan^{-1} \sqrt{x^2 - 1}\, dx}{\sqrt{L^2 - 1} - \sqrt{L^2 - x^2}} \qquad (29)$$

The integral in Eq. (29) is defined as $\Phi(L,\xi)$ and must be integrated numerically[11]. Values of Φ for L ranging from 1.1 to 20 are shown in Fig. 5 to illustrate how Φ behaves as L and ξ are varied.

The total heat flow rate across the sphere-flat contact plane is according to Eq. (29)

$$Q_t = Q_c [1 + 2 k_g^* \Phi(L,\xi)] \qquad (30)$$

where k_g^* is the dimensionless gas conductivity. The overall resistance of the sphere-flat contact, including the effect of a gas, is defined as the overall temperature drop across the contact divided by the total heat flow rate. The overall temperature drop is assumed to be the product of the heat flow rate through the contact area and the constriction resistance under vacuum conditions. Thus we have

$$R_t = \frac{R_c}{1 + 2 k_g^* \Phi(L,\xi)} \qquad (31)$$

where R_c is given by Eq. (8). The effect of radiation can be taken into consideration by simply putting Eq. (16) in parallel with Eq. (31). After normalizing Eq. (31) we obtain for the coupled model with radiation

$$\frac{1}{R_t^*} = \frac{1 + 2 k_g^* \Phi(L,\xi)}{L} + \frac{1}{R_r^*} \qquad (32)$$

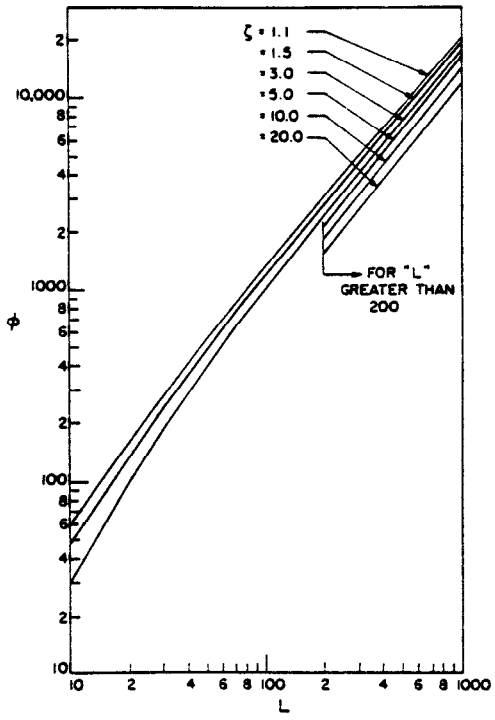

Fig. 5 Coupled model parameter versus dimensionless load parameter

Thermal Resistance With Oil Under Vacuum Conditions

Consider the heat transfer across a sphere-flat contact under vacuum conditions with oil having a thermal conductivity k_o occupying the gap region between $\xi > 1$ and $\beta < L$, Fig. 6. Utilizing

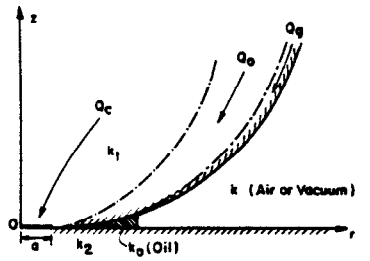

Fig. 6 Model for oil and gas resistance

the decoupled model described above, the total resistance of the oil can be evaluated by means of the following expression:

$$\frac{1}{R_o} = k_o D \frac{\pi}{L} \int_{\xi}^{\beta} \frac{x \, dx}{\sqrt{L^2 - 1} - \sqrt{L^2 - x^2}} \qquad (33)$$

The oil resistance can be normalized using the harmonic mean thermal conductivity k_s. Thus Eq. (33) becomes

$$\frac{1}{R_o^*} = \frac{1}{D \, k_s R_o} = k_o^* \, G_o \, (L, \beta, \xi) \qquad (34)$$

where $k_o^* \equiv k_o / k_s$ and the integral $G_o(L,\beta,\xi)$ is given by

$$G_o(L,\beta,\xi) = \frac{\pi}{L} \left\{ \sqrt{L^2 - 1} \ln \left[\frac{\sqrt{L^2 - 1} - \sqrt{L^2 - \beta^2}}{\sqrt{L^2 - 1} - \sqrt{L^2 - \xi^2}} \right] + \sqrt{L^2 - \beta^2} - \sqrt{L^2 - \xi^2} \right\} \qquad (35)$$

Typical values of $G_o(L,\beta,\xi)$ are shown in Figs. 7-9.

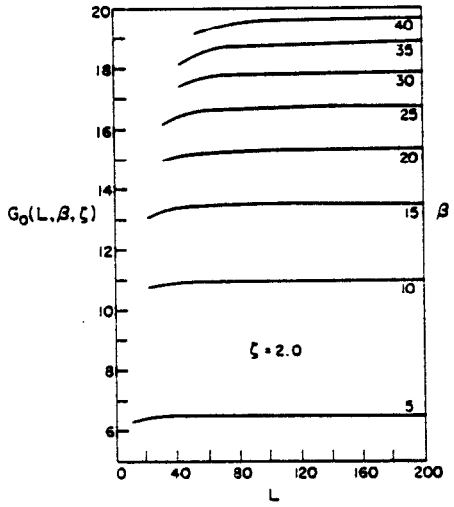

Fig. 7 Oil constriction parameter for $\xi = 2.0$

The lower limit $\xi > 1$ has been used because it is uncertain whether the oil can occupy the gas gap region adjacent to the contact area, especially when the oil is added to sphere-flat contacts under atmospheric conditions. It is assumed that some air is always trapped during the addition of the oil, and this air remains in the region $\xi = 1$ to $\xi > 1$ under vacuum conditions. If one assumes that the presence of the oil does not greatly alter the flow pattern within the solid, Fig. 6, then as a first approximation it can be assumed that the constriction resistance with oil is essentially the same as the constriction resistance without oil. Therefore the total resistance with oil, after non-dimensionalizing, is simply

$$\frac{1}{R_t^*} = \frac{1}{R_c^*} + \frac{1}{R_o^*}$$

$$= (1/L) + k_o^* \, G_o \, (L,\beta,\xi) \qquad (36)$$

Radiative effects can be considered by simply connecting in parallel a modified radiative resistance because the oil is normally opaque and obscures a certain portion of the contact plane.

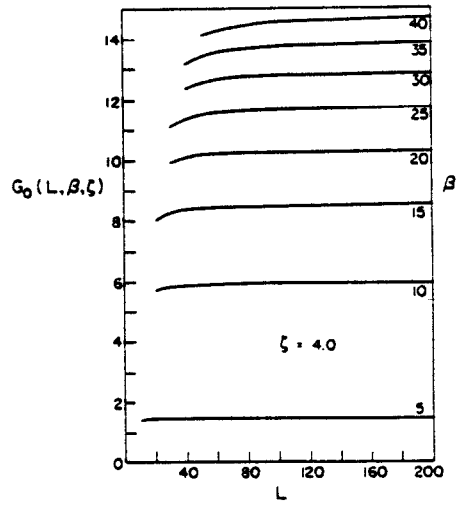

Fig. 8 Oil constriction parameter for $\xi = 4.0$

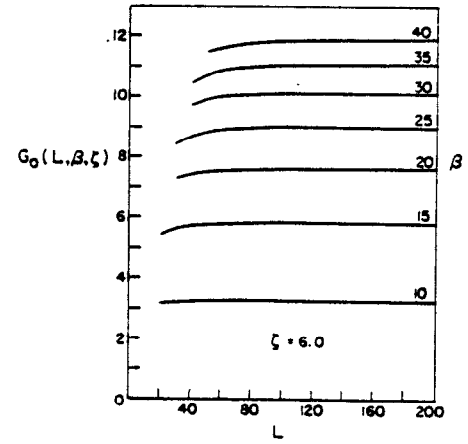

Fig. 9 Oil constriction parameter for $\xi = 6.0$

Thermal Resistance With Oil Under Continuum Conditions

In this analysis it is assumed that oil occupies the gap region between $x = \xi$ and $x = \beta$ while air considered to be a continuum occupies the region between $x = \beta$ and $x = L$. The gap region adjacent to the contact area may be filled with a gas which does not contribute to the heat transfer across the sphere-flat contact. The constriction resistance is assumed to be equal to the

constriction resistance under vacuum conditions with no oil present. The decoupled model will be assumed. The solid, air and oil resistances are thermally connected in prallel and are given by Eqs. (9), (23) and (34), respectively; and therefore the dimensionless total resistance is given by

$$\frac{1}{R_t^*} = \frac{1}{L} + k_g^* G_1 (L,\beta) + k_o^* G_o (L,\beta,\xi) \qquad (37)$$

where G_1 and G_o are defined by Eqs. (24) and (35), respectively. If radiative effects are important, a modified radiative resistance can be connected in parallel with the total resistance given above.

Thermal Resistance in the Slip and Transition Regimes[13, 14]

The continuum regime is characterized by very small Knudsen numbers. In this regime molecular interactions predominate and the temperature within a gas layer bounded by infinite parallel, isothermal walls varies linearly within the gas and the temperature of the gas adjacent to the walls has the same temperature as the walls. When the gas pressure is reduced, the mean free path of the gas increases according to Eq. (21). When the Knudsen number is slightly smaller than unity, the gas far from the walls can still be considered as a continuum with the gas temperature still varying linearly, but adjacent to both walls there is a thin region in which the gas will not have the same temperature as the walls; there will be a temperature discontinuity between the gas and wall because the gas molecules are not able to come into thermal equilibrium with the wall molecules. This regime is often called the slip flow regime. If the gas pressure is reduced even further, the mean free path increases and becomes comparable to the gas thickness. In this regime molecular interactions and molecular/wall interactions are equally frequent. This means that the gas molecules in the vicinity of the wall are influenced by the wall, by the gas molecules in the middle of the layer as well as gas molecules leaving the other wall. In this transition regime, there is a temperature discontinuity at both walls as well as large temperature gradients within the gas adjoining the walls. This temperature gradient decreases in magnitude as one moves from either wall toward the center of the gas layer.

Heat transfer through the gas layer under the conditions described above is usually handled by considering the gas to have an effective thermal conductivity related to the conductivity under continuum conditions in the following manner:[13]

$$k_g = \frac{k_{g\infty}}{1 + 1.67 \frac{\Lambda_\infty}{D_e} \left(\frac{T}{288}\right)\left(\frac{760}{P_g}\right)\left[\frac{2-\alpha_1}{\alpha_1} + \frac{2-\alpha_2}{\alpha_2}\right]} \qquad (38)$$

where D_e is the gas layer thickness, T and P_g are the average gas temperature and pressure, and α_1 and α_2 are the accommodation coefficients between the gas and wall. Eq. (38) is strictly valid for a diatomic gas bounded by infinitely large, parallel, isothermal walls. As a first approximation it will be assumed that Eq. (38) can be used to predict the effect of local slip and transition regime conditions. Using the decoupled model, Eq. (22), the total gas resistance can be evaluated as follows:

$$\frac{1}{R_g} = \int_{r>a}^{L} \frac{k_{g\infty}\, 2\pi r dr}{\delta\left[1 + 1.67 \frac{\Lambda_\infty}{\delta} \frac{T^*}{P_g^*} \alpha\right]} \qquad (39)$$

where δ is the local gas gap thickness and α is the accommodation parameter. The lower limit of integration will be $x = \xi > 1$, corresponding to Knudsen numbers which are equal to about 10. After non-dimensionalizing and integrating one obtains the following expression:

$$\frac{1}{R_g^*} = k_{g\infty}^* G_2 (L,\beta,\xi) \qquad (40)$$

where the integral $G_2 (L,\beta,\xi)$ is defined as

$$G_2 (L,\beta,\xi) = \frac{\pi}{L}\left\{-\sqrt{L^2 - \xi^2} + \left[\sqrt{L^2 - 1} + (3.34\,\alpha\, L)\cdot \Lambda_\infty^* T^*/P_g^*\right]\cdot \ln\left(\frac{\sqrt{L^2 - 1} + 3.34\alpha\, L\, \Lambda_\infty^* T^*/P_g^*}{\sqrt{L^2 - 1} + 3.34\alpha\, L\, \Lambda_\infty^* T^*/P_g^* - \sqrt{L^2 - \xi^2}}\right)\right\} \qquad (41)$$

where $\Lambda_\infty^* = \Lambda_\infty/D$. Eq. (41) reduces to Eq. (24) when $P_g^* = 1$ and $\beta = L$.

The total resistance of a sphere-flat contact in the slip or transition regimes can now be expressed in the following dimensionless form:

$$\frac{1}{R_t^*} = \frac{1}{L} + \frac{1}{R_r^*} + k_{g\infty}^* G_2 (L,\beta,\xi) \qquad (42)$$

where the first two terms on the right-hand side of Eq. (42) are the constriction and radiative resistances, respectively. All three resistances are assumed to be independent.

The presence of oil can be easily taken into account by simply putting the oil resistance in parallel with the constriction and gas resistances. If the oil occupies the gas gap region between $x = \xi$ and $x = \beta$, and the gas is in the slip or transition regimes between $x = \beta$ and $x = \gamma < L$, then the total resistance can be evaluated by means of the following expression:

$$\frac{1}{R_t^*} = \frac{1}{L} + k_o^* G_o (L,\beta,\xi) + k_{g\infty}^* G_2 (L,\gamma,\beta) \qquad (43)$$

Comparison Between Theory and Test Results

The total resistance expressions developed in this paper are compared with test data[11, 12] obtained with smooth, polished hemispheres having diameters of 2.54 and 5.08 cm, respectively. The flats had a rms roughness of 0.12μ. The

mechanical load on the contact ranged from 1.64 to 47.7 kg. The gases used in the tests were air and argon. The gas pressure ranged from 10^{-6} mm Hg to 760 mm Hg. Vacuum oil was used to verify the analysis based upon oil being present in a portion of the gap. The temperature of the interface ranged from 304°K to 332°K. All tests were conducted during the first loading cycle. The elastic properties of the hemispheres and flat were identical; the modulus of elasticity was 2.11 x 10^6 kg/cm^2 and Poisson's ratio was taken to be 0.30. The thermal conductivities of the hemispheres were determined to be 0.50 and 0.41 W/cm°K for the 2.54 cm and 5.08 cm test specimens, respectively. The emissivities of the 2.54 cm hemisphere-flat tests were assumed to be 0.1 and 0.9 respectively[11]. For the 5.08 cm hemisphere-flat tests, the emissivities were taken to be 0.3 and 0.8, respectively. These values are not critical because the radiative resistances were very large. It was assumed that the accommodation coefficients for the air tests were 0.87 and 0.92[11]. For the argon tests these values were taken to be 0.90 and 0.90. Continuum conditions were assumed to exist within the gas gap ($\xi > 1$) for all pressures greater than 100 mm Hg. The slip and transition analysis was assumed to be valid in the pressure range from 0.1 mm to 100 mm Hg.

Fig. 10 shows the excellent agreement over the entire load range between the vacuum test data including radiative effects for the two test specimens and the theory, Eq. (18). It is remarkable that the excellent agreement for the first loading cycle, persists down to L = 35.4 where the flat has experienced substantial plastic deformation[15].

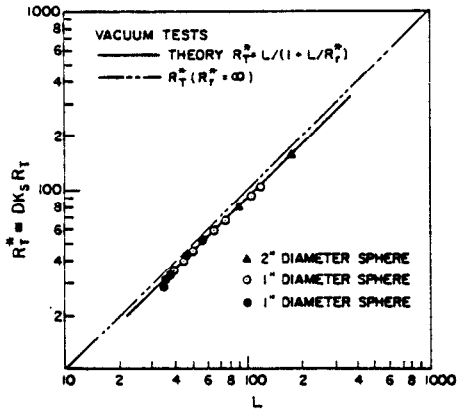

Fig. 10 Comparison of constriction theory and test data

The excellent agreement between both decoupled and coupled models under continuum conditions; Eqs. (18) and (23) for the decoupled system, and Eq. (32) for the coupled as shown in Tables 1 - 5 for the 2.54 cm hemisphere with air and argon present in the gas gap.

Table 1 Predicted R_c^* and R_g^* for Air and D = 2.54 cm. Decoupled Model

L	R_c^*	R_g^* ξ = 2.5	3.0	3.5
115.1	108.8	79.0	83.7	87.9
103.2	98.1	81.4	86.3	90.8
76.0	73.3	89.1	95.1	100.5
65.4	63.3	93.2	99.8	105.8
50.0	48.8	102.1	110.0	117.3
45.1	44.1	105.6	114.0	122.0
37.4	36.7	113.3	123.1	132.4

Table 2 Comparison Between Theory and Test for Air and D = 2.54 cm. Decoupled Model

L	R_t^*(test)[11]	R_t^*(theory) ξ = 2.5	3.0	3.5
115.1	47.5	45.8	47.3	48.6
103.2	45.0	44.5	45.9	47.2
76.0	42.1	40.2	41.4	42.4
65.4	37.3	37.3	38.8	39.6
50.0	34.4	33.0	33.8	34.5
45.1	32.5	31.1	31.8	32.9
37.4	27.3	27.7	28.3	28.8

Table 3 Predicted R_g^* for Air and D = 2.54 cm. Coupled Model

L	R_g^* ξ = 2.5	3.0	3.5
115.1	80.7	84.2	87.8
103.2	83.8	87.6	91.4
76.0	93.5	98.2	102.9
65.4	98.7	103.9	109.3
50.0	109.9	116.3	123.0
45.1	114.4	121.3	128.6
37.4	123.9	132.0	140.6

Table 4 Comparison Between Theory and Test for Air and D = 2.54 cm. Coupled Model

L	R_t^*(test)[11]	R_t^*(theory) ξ = 2.5	3.0	3.5
115.1	47.5	46.3	47.5	48.6
103.2	45.0	45.2	46.3	47.3
76.0	42.1	41.1	42.0	42.8
65.4	37.3	38.6	39.4	40.1
50.0	34.4	33.8	34.4	31.9
45.1	32.5	31.8	32.3	32.8
37.4	27.3	28.3	28.7	29.1

Table 5 Comparison Between Theory and Test for Air and Argon, D = 2.54 cm. Decoupled Model at $\xi = 3.0$

L	Air			Argon		
	R_t^*(test)[11]	R_t^*(theory)	% Error	R_t^*(test)[11]	R_t^*(theory)	% Error
115.1	47.5	47.3	-0.5	57.8	58.3	0.9
103.2	45.0	45.9	2.1			
76.0	42.1	41.4	-1.9	48.3	48.4	0.0
65.4	37.3	38.8	3.8			
50.0	34.4	33.8	-1.8	39.2	37.7	-4.0
45.1	32.5	31.8	-2.1			
37.4	27.3	28.3	3.7	29.7	30.6	3.1

Tables 1 and 3 contain the predicted values of R_c^* and R_g^* for air based upon the decoupled and coupled models, respectively. Values of R_g^* at three different lower limits ξ are shown for various values of L which ranged from 115.1 to 37.4. It will be noted that for corresponding values of ξ there is a slight difference between the decoupled and coupled models. The difference is least at the smallest mechanical loads, and is the greatest at the largest mechanical loads. The difference between the two models also decreases with increasing ξ. Tables 2 and 4 show the comparison between total resistance test data for air and the predicted values of total resistance based upon the decoupled and coupled models. It can be seen that the two models yield comparable values for the three values of the lower limit ξ. Excellent agreement is observed between the total resistance test data for both air and argon and the predicted values based upon the decoupled model at $\xi = 3.0$, Table 5. It can be seen that the maximum error is -4.0% which occurs at L = 50.0 for the argon test. A slightly better agreement is observed between the test data and the coupled model theory at $\xi = 3.0$.

Test data[11] for the 5.08 cm hemisphere were obtained with air and argon, and it can be reported that there was excellent agreement between the tests and the predicted values based upon the decoupled and coupled models when $\xi = 4.0$. This is consistent with the predicted values of ξ based upon Eq. (20), which shows clearly that for a larger curvature, ξ will be greater because L will be larger for the same mechanical load.

Table 6 shows the comparison between some test data with oil present under atmospheric conditions and the decoupled model, Eq. (37). Radiative effects were negligible and therefore not considered. It can be seen that there is a very good agreement when the lower limit for the oil resistance is in the range 3.0 to 4.0 for the 2.54 cm test specimen and in the range 4.0 to 4.5 for the 5.08 cm specimen. The upper limit for the oil was determined photographically. It can be seen that the oil resistance is quite sensitive to the parameter ξ because the percent error changes from negative values for the smaller value of ξ to positive values for the larger value. The fact that all three tests indicate the same values of the lower limit ξ is consistent with the manner in which the oil was added to the test specimens[11] The gap region adjacent to the contact area was occupied by trapped air when the oil was added. Surface tension prevented the oil from completely wetting the hemisphere and flat in the gap region $1 < \xi < 3$ to 4.

In Table 7 one can see the comparison between theory and test under vacuum conditions corresponding to 10^{-6} mm Hg when the gas conduction is negligible. Since the radiative effects are negligible, only solid constriction resistance and oil resistances are present. The total resistance, Eq. (36), is a function of L, β, ξ and k_o^*.

It can be seen that when the gas is not present the total resistance is quite sensitive to the lower limit ξ. For example, the percent error changes from -6.2 to 4.5 as ξ goes from 3.5 to 4.5 in the first test. Similar observations were made with the other tests. The vacuum test results are consistent with the continuum test results in the fact that the same values of the lower limit ξ yield the best agreement between theory and test. As expected the presence of oil makes the total resistance less sensitive to the gas pressure. With oil present the total resistance changes by about 10% as the gas pressure is reduced from atmospheric to vacuum conditions. On the other hand, without oil, the total resistance is very sensitive to the gas pressure, depending upon the magnitude of the constriction resistance.

The predicted total resistance, Eqs. (41) and (42), in the slip and transition regimes without oil in the gap is compared with the air and argon test data in Table 8. In the comparison it is assumed that the predicted values of resistance are valid for gas pressures ranging from about 0.10 to 100 mm Hg. Very good agreement is obtained for air and argon for both sizes of spheres over the load range L = 37.4 to 179.5 when the lower limit ξ is in the range of 2 to 5. In this range of ξ, the local pseudo-Knudsen number varies from about 0.02 to 30 depending upon L and P_g for all the tests conducted. For the majority of tests Kn ranges between 0.1 and 10.

Conclusions

Decoupled and coupled models are presented for predicting the overall thermal resistance of a sphere-flat contact with and without oil over the gas pressure range from vacuum to atmospheric conditions. There is excellent agreement between theory and test data for air and argon gas. The simple decoupled model is shown to be comparable to the more complex coupled model over the entire load range for both air and argon under continuum conditions. Elasticity theory can be used to predict the contact area and the constriction resistance during the first loading cycle up to a relative contact of 3%, at which point both the sphere and flat have undergone plastic deformation.

Table 6 Comparison Between Theory and Test Data with Oil Under Continuum Conditions. Decoupled Model.

D	L	β	ξ	R_c^*	R_g^*	R_o^*	R_t^*	R_t^*	% Error
cm							Eq. (37)	Test[11]	
2.54	65.4	18.0	3.5	63.4	260.8	36.8	21.4	22.2	-3.8
	65.4	18.0	4.0	63.4	260.8	40.3	22.5	22.2	1.4
2.54	45.1	8.7	3.0	44.1	199.6	55.0	21.8	22.3	-2.5
	45.1	8.7	3.5	44.1	199.6	64.9	23.2	22.3	3.7
5.08	93.4	12.3	4.0	90.1	211.3	47.8	27.2	28.0	-3.3
	93.4	12.3	4.5	90.1	211.3	53.5	29.0	28.0	3.5

Table 7 Comparison Between Theory and Test Data with Oil Under Vacuum Conditions. Decoupled Model

D	L	β	ξ	R_c^*	R_g^*	R_o^*	R_t^*	R_t^*	% Error
cm							Eq. (36)	Test[11]	
2.54	65.4	18.0	3.5	63.1	∞	37.2	23.4	24.8	-6.2
			4.0	63.1	∞	40.7	24.7	24.8	-0.5
			4.5	63.1	∞	44.3	26.0	24.8	4.5
2.54	65.4	8.7	3.0	43.9	∞	55.5	24.5	26.0	-5.8
			3.5	43.9	∞	65.5	26.3	26.0	1.3
			4.0	43.9	∞	77.2	28.0	26.0	7.3
5.08	93.4	12.3	3.5	89.6	∞	42.8	29.0	31.0	-7.1
			4.0	89.6	∞	48.1	31.3	31.0	1.0
			4.5	89.6	∞	54.0	33.7	31.0	8.0

Table 8 Comparison Between Theory and Test Data. Slip and Transition Regimes.

D	Gas	L	P_g	ξ	Kn	R_c^*	R_g^*	R_t^*	R_t^*	% Error
cm			mm Hg					Eq. (42)	Test[11]	
2.54	Argon	115	80.0	2.0	0.482	108.5	126.6	58.4	58.5	-0.7
				5.0	0.062	108.5	153.0	63.5	58.5	7.3
		76	20.0	2.0	0.838	73.1	153.7	49.5	51.7	-4.4
				5.0	0.105	73.1	183.9	52.3	51.7	1.1
		50	20.0	2.0	0.361	48.7	161.2	37.4	39.3	-5.2
				5.0	0.045	48.7	213.0	39.6	39.3	0.7
		115	10.0	2.0	3.875	108.4	165.2	65.4	62.8	4.1
				5.0	0.484	108.4	178.9	67.5	62.8	7.0
		115	4.9	2.0	7.950	108.3	190.9	69.1	67.8	1.6
				5.0	0.993	108.3	199.1	70.1	67.8	3.3
		37.4	3.0	2.0	1.353	36.7	221.9	31.5	31.2	1.0
				5.0	0.169	36.7	271.3	32.3	31.2	3.5
		76	2.4	2.0	7.06	73.0	225.0	55.1	57.2	-3.8
				5.0	0.88	73.0	238.0	55.9	57.2	-2.5
		76.0	0.7	2.0	24.4	72.9	315.9	59.2	59.5	-0.4
				5.0	3.05	72.9	323.7	59.5	59.5	0.0
		103.0	1.1	2.0	27.32	97.7	189.5	64.4	63.3	1.8
				5.0	3.413	97.7	193.1	64.4	63.3	2.4
		50.0	0.7	2.0	10.06	48.7	218.9	39.8	40.9	-2.6
				5.0	1.255	48.7	231.6	40.2	40.9	-1.6
		45.1	0.45	2.0	12.73	44.0	254.4	37.5	37.6	-0.3
				5.0	1.587	44.0	268.2	37.8	37.6	0.4
		115.0	0.20	2.0	190.2	108.2	350.6	82.5	80.3	2.7
				5.0	23.76	108.2	352.4	82.6	80.3	2.8

5.08	Air	179.5	20.0	5.0	0.281	166.9	111.3	66.8	73.7	-10.3
				10.0	0.068	166.9	136.1	75.0	73.7	1.7
		89.7	20.0	2.0	0.555	86.5	106.0	47.6	51.2	-7.4
				5.0	0.069	86.5	135.9	52.9	51.2	3.2
		89.7	2.8	2.0	3.996	86.4	154.7	55.4	58.9	-6.2
				5.0	0.499	86.4	171.0	57.4	58.9	-2.6
		179.5	2.3	5.0	2.478	166.4	178.2	82.8	89.9	-8.1
				10.0	0.600	166.4	226.7	86.1	89.9	-4.1
		179.5	0.8	5.0	7.18	166.1	229.5	96.4	108.2	-12.2
				10.0	1.74	166.1	239.4	98.1	108.2	-10.3
		89.7	0.625	2.0	18.09	86.3	250.6	64.2	67.2	-4.6
				5.0	2.26	86.3	261.3	64.9	67.2	-3.5
		50.0	0.4	2.0	18.39	48.7	358.9	43.2	43.2	-0.1
				5.0	2.29	48.7	401.5	43.4	43.2	0.3
2.54	Air	50.0	70.0	2.0	0.098	35.9	97.6	32.5	35.9	-10.3
				5.0	0.012	35.9	139.3	36.0	35.9	0.5
		115.0	40.0	2.0	0.920	108.6	94.0	50.4	52.4	-3.8
				5.0	0.115	108.6	109.0	54.4	52.4	3.8
		103.0	20.0	2.0	1.480	97.9	103.6	50.3	50.7	-0.8
				5.0	0.185	97.9	117.2	53.3	50.7	4.9
		50.0	20.0	2.0	0.344	48.7	110.9	33.9	37.0	-9.2
				5.0	0.043	48.7	146.8	36.6	37.0	-1.0
		45.1	20.0	2.0	0.282	44.0	112.6	31.7	34.1	0.3
				5.0	0.035	44.0	153.1	34.2	34.1	7.5
		37.4	20.0	2.0	0.193	36.7	116.8	27.9	29.3	-4.8
				5.0	0.024	36.7	167.3	30.1	29.3	2.8
		76.0	10.0	2.0	1.600	73.2	117.1	45.0	43.7	3.0
				5.0	0.200	73.2	133.8	47.3	43.7	7.7
		65.4	10.0	2.0	1.186	63.3	118.1	41.2	39.9	3.2
				5.0	0.148	63.3	139.0	43.5	39.9	8.3
		115.0	5.0	2.0	7.429	108.2	131.2	59.4	58.2	2.0
				5.0	0.928	108.2	137.1	60.5	58.2	3.8

Acknowledgements

The authors acknowledge the financial support of the National Research Council of Canada. One of the authors (W. W. K.) acknowledges the assistance of Professor I. J. McGee of the Department of Applied Mathematics, and Professors C. E. Hermance and K. G. T. Hollands of the Department of Mechanical Engineering.

References

1 JANSSON, R.M., "The Heat Transfer Properties of Structural Elements for Space Instruments", Report E-1173, Instrumentation Laboratory, Mass. Inst. of Technology, Cambridge, June 1962.

2 YOVANOVICH, M.M., "Thermal Contact Resistance Across Elastically Deformed Spheres", Journal of Spacecraft and Rockets, Vol. 4, No. 1, Jan. 1967, pp. 119-122.

3 YOVANOVICH, M.M., "Analytical and Experimental Investigation of the Thermal Resistance of Angular Contact Instrument Bearings", Instrumentation Laboratory Report E-2215, Mass. Inst. of Technology, December 1967.

4 YOVANOVICH, M.M., "Thermal Constriction Resistance Between Contacting Metallic Paraboloids: Application to Instrument Bearings", AIAA Paper 70-857, AIAA 5th Thermophysics Conference, Los Angeles, Calif., June 29 - July 1, 1970. Heat Transfer and Spacecraft Thermal Control, Prog. Aeronautics and Astronautics, Vol. 24, Editor J. W. Lucas, 1970.

5 SEELY, F.B. and SMITH, J.O., Advanced Mechanics of Materials, Wiley, New York, 1963, Chap. 11.

6 CAMERON, A., The Principles of Lubrication, Wiley, New York, 1966, 1st Edition.

7 YOVANOVICH, M.M., CORDIER, H. and COUTANCEAU, J., "Sur la resistance due a un contact unique de section circulaire", Comptes Rendus de l'Academie Sciences, Paris, Vol. 268, Jan. 6, 1969, pp. 1-4.

8 HOLM, R., Electric Contacts, Theory and Applications, 4th Edition, Springer-Verlag, New York Inc., 1967.

9 KREITH, F., Principles of Heat Transfer, 2nd Edition, International Textbook Company, 1969.

10 SIEGEL, R. and HOWELL, J.R., Thermal Radiation Heat Transfer, 1st Edition, McGraw-Hill Inc., 1972.

11 KITSCHA, W.W., M.A.Sc. Thesis, Department of Mechanical Engineering, University of Waterloo, March 1973.

12 KITSCHA, W.W. and YOVANOVICH, M.M., "Experimental Investigation on the Overall Thermal Resistance of a Sphere-Flat Contact", In preparation.

13 KENNARD, E.H., Kinetic Theory of Gases, McGraw-Hill, New York, 1938, pp. 315-320.

14 SCHAAF, S.A., "Heat Transfer in Rarefied Gases", Chapter 7, Developments in Heat Transfer, Edited by W.M. Rohsenow, MIT Press, 1964.

15 STOREY, C., "Investigation into One of the Assumptions of the Hertz Theory of Contact", British Journal of Applied Physics, Vol. 11, Feb. 1960.